

Ferroresonance Conditions in Wind Parks

U. Karaagac, J. Mahseredjian, L. Cai

Abstract--Wind parks are made up of a large number of saturable inductances (power transformers, inductive voltage transformers (IVTs)), as well as capacitors (cables, wind turbine harmonic filters, capacitor voltage transformers (CVTs), voltage grading capacitors in circuit-breakers). Therefore, they may present scenarios in which ferroresonance occurs. This paper presents the scenarios that can lead to ferroresonant circuits in doubly fed induction generator (DFIG) based wind parks. Ferroresonance conditions and their consequences are demonstrated by simulating the detailed model of the wind park in EMTP-RV. The wind park simulation model includes detailed models of wind turbines, medium voltage (MV) collector grid, high voltage / medium voltage (HV/MV) wind park substation, overvoltage, overcurrent and differential current protections, current transformers (CTs), IVTs and CVTs.

Keywords: Ferroresonance, wind parks, power transformers, inductive voltage transformers (IVTs), capacitor voltage transformers (CVTs), overvoltage, overcurrent.

I. INTRODUCTION

FERRORESONANCE is an oscillatory phenomena caused by the interaction of energy exchanged between the nonlinear magnetizing inductances of the ferromagnetic cores and the system capacitances. The main feature of this phenomenon is the presence of at least two stable steady-state operating points for a particular range of circuit parameters: a ferroresonant operating point and a normal (non-ferroresonant) operating point. Transient disturbances or switching operations may initiate ferroresonance. The response can suddenly jump from one normal operating point (sinusoidal at the same frequency as the source) to another ferroresonant operating point characterized by high overvoltages and harmonic levels which may lead to excessive heating and insulation failure in transformers as well as significant disruptions in power system operation [1], [2].

This paper presents the scenarios that can lead to ferroresonant circuits in an actual doubly fed induction generator (DFIG) based wind park. Ferroresonance conditions and their consequences are demonstrated by simulating the detailed model of the wind park in EMTP-RV.

This work was supported by the German Federal Ministry for the Environment, Nature Conservation, Building and Nuclear Safety, grant code: 032529.

U. Karaagac and J. Mahseredjian are with École Polytechnique de Montréal, Campus Université de Montréal, 2900, Édouard-Montpetit, Montréal (Québec), Canada, H3T 1J4.

L. Cai is with Senvion SE, Überseering 10, D-22297, Hamburg, Germany.

Paper submitted to the International Conference on Power Systems Transients (IPST2015) in Cavtat, Croatia June 15-18, 2015

The first part of this paper presents the theoretical principles of ferroresonance. The second part presents the considered wind park and the electric configurations that can lead to ferroresonant circuits. The simulation results are presented in the last part.

II. FERRORESONANCE

In simple terms, ferroresonance can be described as a nonlinear oscillation resulting from the interaction between a nonlinear inductance and a capacitor. Like linear resonance, depending on the connection between the capacitance and the nonlinear inductance, ferroresonance may be series or parallel. This paper analyzes only the series ferroresonance shown in Fig. 1.

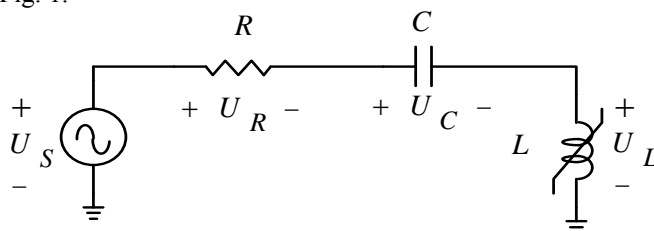


Fig. 1. Series ferroresonant circuit.

The graphical solution of the series resonant circuit is shown in Fig. 2 for the lossless case (i.e. $R = 0$). The intersection of " $U_S + U_C$ " line with the nonlinear $U_S(I)$ curve gives three possible operating points:

- Operating point (1): Non-ferroresonant stable operating point in which the circuit is working in an inductive mode, with lagging current and low voltages.
- Operating point (2): Ferroresonant stable operating point in which the circuit is working in a capacitive mode, with leading current and high voltages.
- Operating point (3): Unstable operating point.

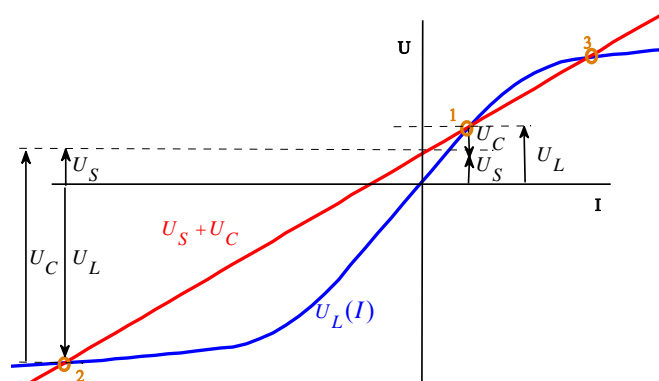


Fig. 2. Graphical solution of a series ferroresonant circuit ($R = 0$).

It should be noted that, the deep analysis of the circuit shown in Fig. 1 requires the solution of nonlinear differential equations. The presence of nonlinearity introduces harmonics in the voltage and current waveforms. However, in Fig.2, the analysis of the circuit is simplified by limiting the calculations to the power frequency and steady state in order to provide a conceptual description of ferroresonance [3]-[5].

A. Effect of Source Voltage

The effect of the source voltage is illustrated in Fig. 3. As the source voltage is increased, the “ $U_S + U_C$ ” line moves upwards. When the source voltage is higher than $U_{S-critical}$ (“ $U_S + U_C$ ” line tangent to the nonlinear $U_S(I)$ curve), there is no intersection in the first quadrant. In other words, the system solution is always a ferroresonant situation.

As seen from Fig. 3, the ferroresonant oscillations can be self-sustained when the circuit has no losses. In other words, removing voltage source may not result in the elimination of ferroresonance. The operating point simply slides to the right, but remains in the saturated region. In reality, ferroresonant oscillations cannot be self-sustained due to circuit losses.

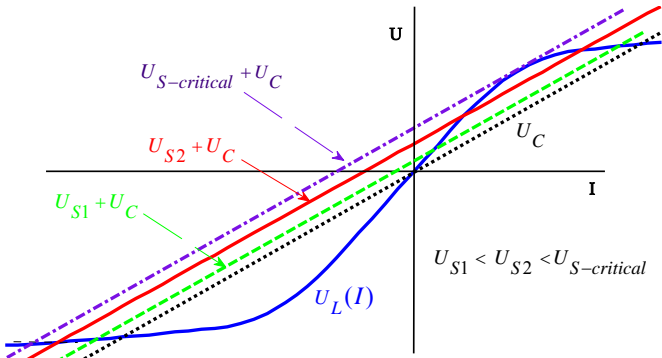


Fig. 3. Graphical solution illustrating the effect of source voltage.

B. Effect of Circuit Capacitance

The effect of the circuit capacitance is illustrated in Fig. 4. As the circuit capacitance is increased, the “ $U_S + U_C$ ” line rotates clock-wise, i.e. its slope decreases. As seen from Fig. 4, ferroresonant situation can appear for a wide range of capacitance values at a given frequency.

Fig. 5 illustrates the theoretical conditions to avoid periodic ferroresonance. It can be observed when [1]

$$\omega L_{sat} < \frac{1}{\omega C} < \omega L_{linear} \quad (1)$$

C. Effect of Circuit Losses

When the losses are considered, the equation describing the steady-state behaviour of the circuit shown in Fig. 1 can be written as

$$|U_L(I) - U_C| = \sqrt{U_S^2 - (R I)^2} \quad (2)$$

The graphical solution is shown in Fig.6. For the low circuit resistance (R_1), there are three possible solutions. Solutions (1) and (2) in Fig.6 correspond to the non-

ferroresonant and the ferroresonant situations, respectively. As seen from Fig.6, the multiplicity of solutions can disappear when the circuit losses increases.

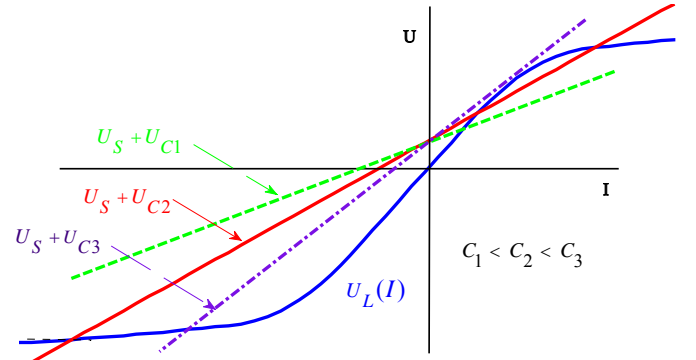


Fig. 4. Graphical solution illustrating the effect of circuit capacitance.

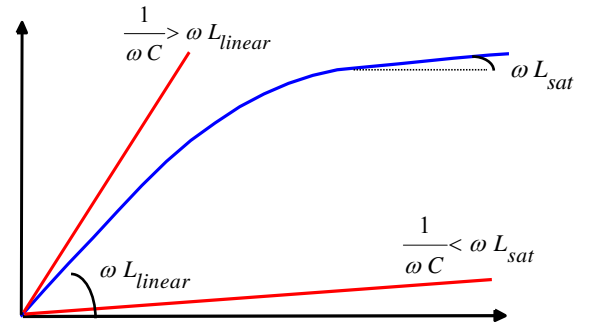


Fig. 5. Periodic ferroresonance conditions.

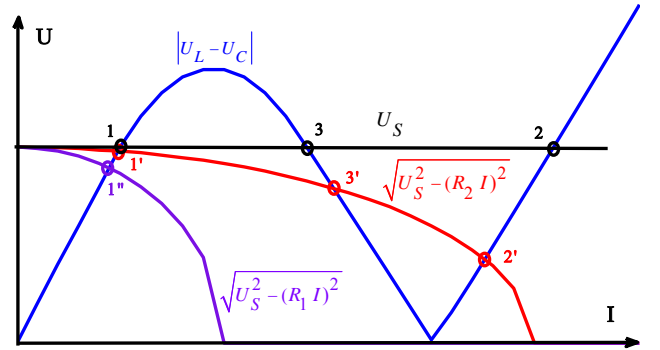


Fig. 6. Graphical solution illustrating the effect of circuit losses ($R_1 > R_2$).

III. WIND PARK UNDER STUDY

The simplified single-line diagram of the wind park studied in this paper is given in Fig. 7. The wind park collector grid is composed of three radial 34.5 kV feeders and connected to 120 kV grid through a 120 MVA step-up transformer. The collector grid feeders F1, F2 and F3 contain 15, 7 and 18 DFIG-type wind turbines (WTs), respectively. Each WT has 2 MW rating and connected to 34.5 kV collector grid through a 2.5 MVA ΔY_g transformer. The EMTP-RV diagram of the wind park substation is given in Fig. 8. The isolating switches are not shown in in Fig. 8. The reader should refer to [6] for detailed information regarding DFIG WTs and wind park control.

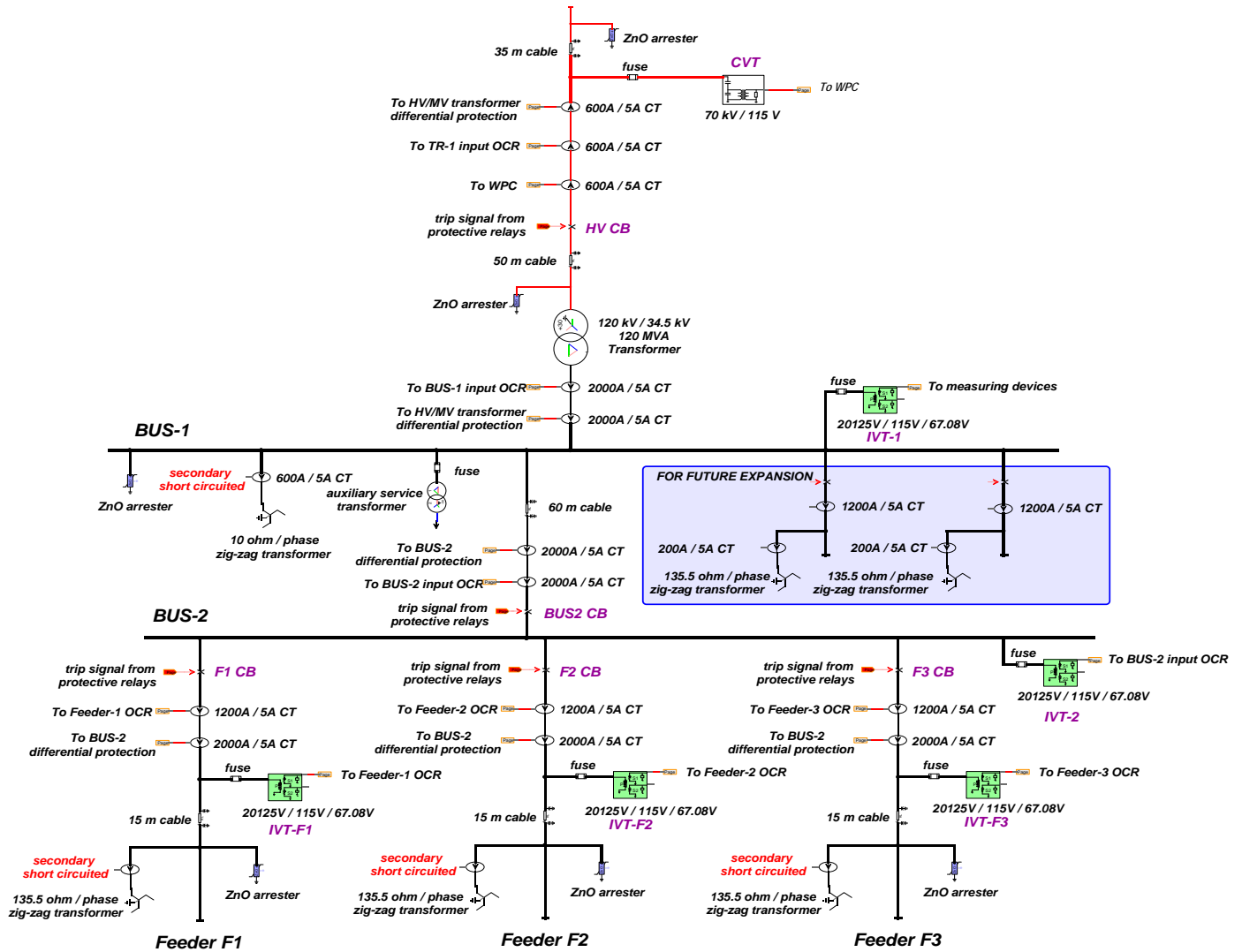


Fig. 8. EMTP-RV diagram of the wind park substation

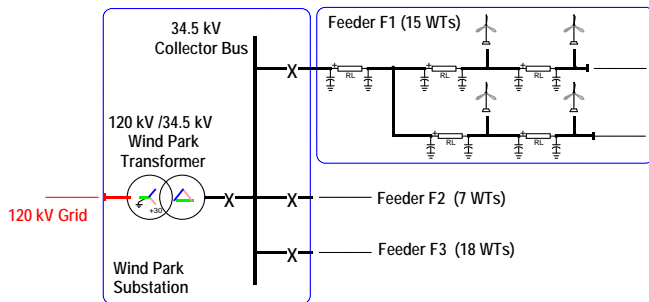


Fig. 7. Simplified single-line diagram of the wind park.

There are several electric configurations that can lead to ferroresonant circuits in power systems. In [7] seven different classes or categories of electrical systems prone to ferroresonance appearance are identified. The following three electric configurations exist in the considered wind park.

1. Transformer supplied accidentally on one or two phases [8]-[10];
2. Inductive voltage transformer (IVT) energized through the grading capacitance of one or more open circuit breakers [11], [12];

3. Capacitor voltage transformer (CVT) [13], [14].

A. Transformer Supplied Accidentally on One or Two Phases

The DFIG transformers have delta primary connection and ferroresonance may occur when they are supplied on one or two phases. The ferroresonant circuit is created through the phase-to ground capacitance(s) of the open phase(s) as shown in Fig. 9. The following scenarios can be expected to cause ferroresonance:

1. Energizing a DFIG transformer (via closing associated MV load break switch) when one or two phases of the feeder cable are live due to a stuck pole or poles in the feeder circuit breaker,
2. Energizing collector grid feeder on one or two phases due to a stuck pole or poles in the feeder circuit breaker when the DFIG transformers (one or more) are connected to the feeder to be energized,
3. A stuck pole (or poles) in the circuit breaker during opening following nuisance operation of the overcurrent relay (OCR).

It should be noted that, the feeder cables and DFIG transformers are energized sequentially during startup. Therefore, the second scenario cannot happen when the startup procedure is followed.

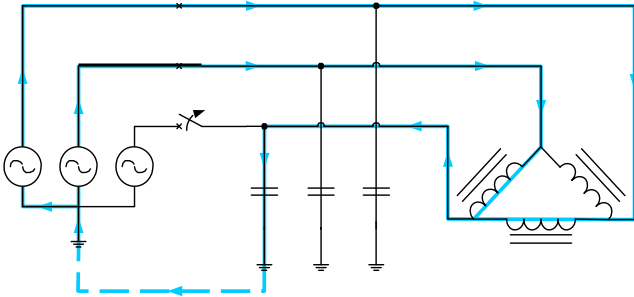


Fig. 9. Ferroresonant circuit in a transformer with delta primary connection [1].

B. Transformer Energized Through the Grading Capacitance of One or More Open Circuit Breakers

This electrical configuration is shown in Fig. 10. Opening of circuit-breaker initiates the phenomenon by causing capacitance C to discharge through the IVT which is then driven into saturation. The source delivers enough energy through the circuit-breaker grading capacitance C_d to maintain the oscillation [11], [15].

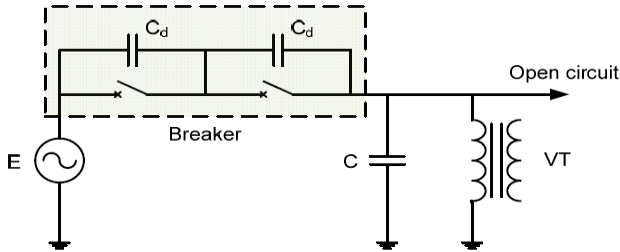


Fig. 10. IVT in series with an open circuit breaker [1].

In the considered wind park, the IVTs may form a ferroresonant circuit with the grading capacitance of circuit-breakers for the following scenarios:

1. BUS2 IVT and BUS2 input circuit breaker grading capacitance (IVT-2 and BUS2 CB in Fig. 8) when 34.5 kV feeders are disconnected;
2. BUS1 IVT and 120 kV wind park transformer input circuit breaker grading capacitance (IVT-1 and HV CB in Fig. 8) when BUS-2 is disconnected.

C. Capacitive Voltage Transformer (CVT)

The structure of CVTs makes them particularly prone to ferroresonance. Manufacturers are aware of this problem and install various types of suppression circuits. These suppression circuits should not affect either the transient response or the accuracy of the transformer, but limiting the duration of the ferroresonant oscillations [16]-[20]. As seen in Fig. 8, the considered wind park has a CVT at 120 kV.

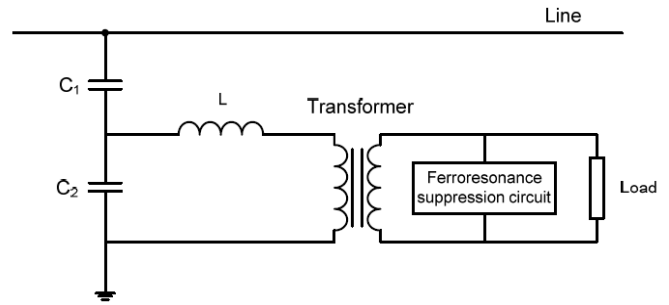


Fig. 11. Capacitive voltage transformer (CVT) [2].

IV. EMTP-RV SIMULATIONS

A. Simulation Model

The simulation model in [6] is used in this study. The model includes detailed models of DFIG WTs, wind park controller, MV collector grid, HV/MV wind park substation, overvoltage protection, overcurrent and differential current protections, current transformers, IVTs and CVTs. It should be noted that, all simulation data is provided by the manufacturer except the circuit breaker grading capacitances.

B. Simulation Results

1) Scenario S1

This scenario is energizing the feeder F1 (at $t = 0.75$ s) on two phases due to a stuck pole (the pole on phase-c) in the feeder F1 circuit breaker (F1 CB in Fig. 8) when all DFIG transformers are connected to the feeder. This scenario is not expected to happen as the feeder cables and DFIG transformers are energized sequentially during startup and presented only to demonstrate the ferroresonance phenomenon.

It should be noted that energizing one of the DFIG transformers with closing the associated MV load break switch does not cause ferroresonance (when one or two phases of the feeder F1 cable is live) even for 1.5 pu voltage at collector grid. In the simulations, such large voltage profile in collector grid is achieved by increasing DFIG output and transmission system equivalent source voltages after deactivating DFIG overvoltage protection and certain controller limits.

The voltages at MV and LV sides of the DFIG-F104 (one of the DFIGs on feeder F1) transformer are shown in Fig. 12 and in Fig. 13, respectively. The high overvoltage at transformer terminals is due to ferroresonance. The voltage waveforms at the other DFIG transformer terminals on feeder F1 are similar to DFIG-F104 transformer terminals. The energy absorptions of the surge arresters at the MV and the LV sides of the DFIG-F104 transformer are given in Fig. 14 and Fig. 15, respectively. As the ferroresonance condition will continue due to low damping (see Fig. 12 and Fig. 13), the energy absorptions of the surge arresters will continue increasing. The DFIG transformers and surge arresters are subjected to this overvoltage.

This ferroresonance condition does not affect the operation of the DFIGs on feeders F2 and F3 as it does not cause overvoltage at their terminals as illustrated in Fig. 16.

The possibility of ferroresonance can be expected to decrease with the decrease in the number of DFIG transformers connected to the feeder to be energized.

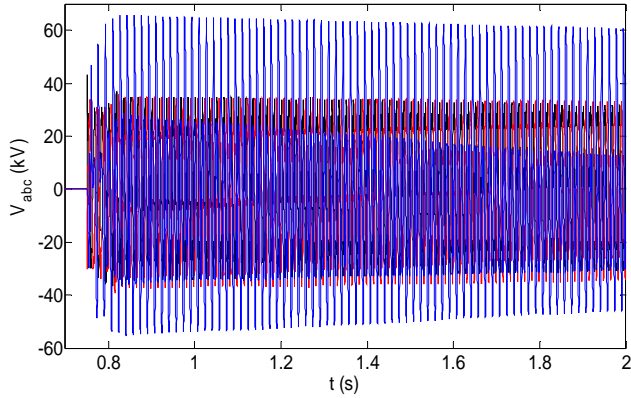


Fig. 12. Voltages at MV side of the DFIG-F104 transformer.

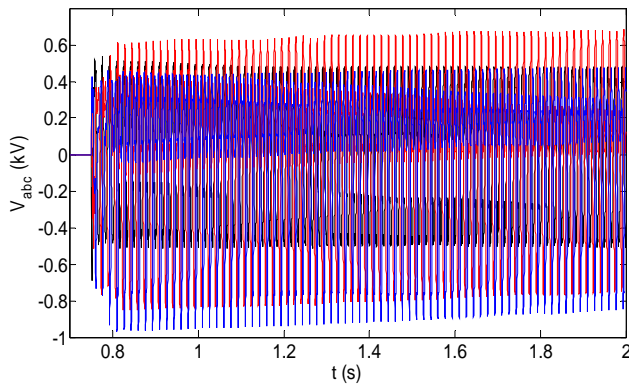


Fig. 13. Voltages at LV side of the DFIG-F104 transformer.

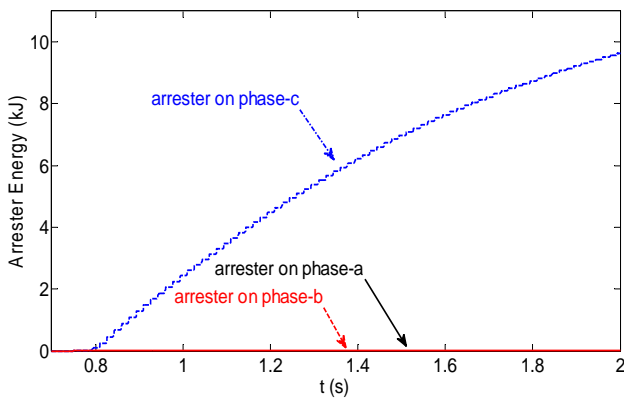


Fig. 14. DFIG- F104 transformer MV arrester energy absorption.

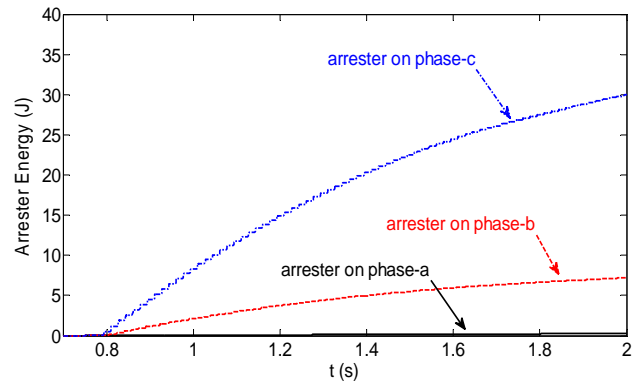


Fig. 15. DFIG- F104 transformer LV arrester energy absorption.

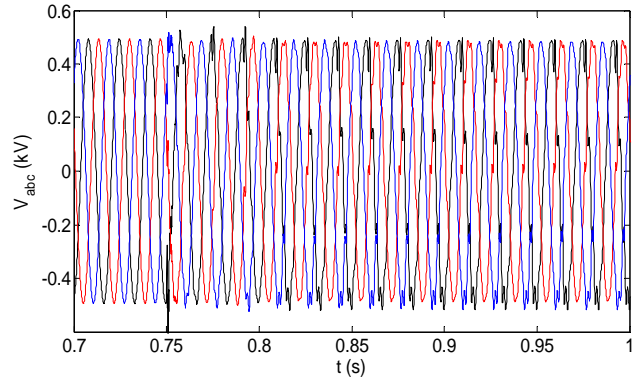


Fig. 16. Voltages at one of the DFIG terminals on feeder F2 (DFIG-F204).

2) Scenario S2:

This scenario is nuisance tripping of feeder F1 OCR and a stuck pole (the pole on phase-c) in F1 CB. F1 CB operates at $t = 0.75$ s in the simulation. The voltages at MV and LV sides of the DFIG-F104 transformer are shown in Fig. 17 and in Fig. 18, respectively. The high overvoltage at transformer terminals is due to ferroresonance condition. DFIG-F104 trips at 0.816 due to operation of overvoltage relay. The energy absorptions of the surge arresters at the MV and the LV sides of the DFIG-F104 transformer are given in Fig. 19 and Fig. 20, respectively. It should be noted that, resonance condition occurs at all DFIG transformers on feeder F1. The voltage waveforms of those DFIGs are similar to DFIG- F104. As the ferroresonance condition will continue, the energy absorptions of the surge arresters will continue increasing. The transformers, surge arresters and line filters of the DFIGs on feeder F1 are subjected to this overvoltage. Similar to the previous simulation scenario, this ferroresonance condition does not affect the operation of the DFIGs on feeders F2 and F3 as it does not cause overvoltage at their terminals.

In Scenario S1, the OCR of feeder F1 and in Scenario S2, the BUS2 input OCR of does not operate due to currents resulting from ferroresonance. The overvoltage in Scenario S2 is much higher than the overvoltage in Scenario S1. It should be noted that, the ferroresonance resulting from nuisance tripping of BUS2 input OCR and a stuck pole in BUS2 CB is much higher than the overvoltage in Scenario S2.

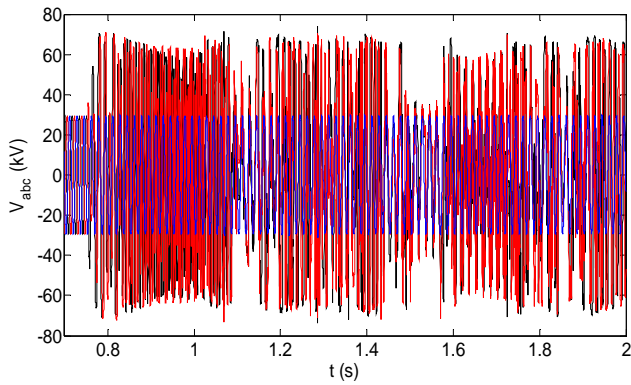


Fig. 17. Voltages at MV side of the DFIG-F104 transformer.

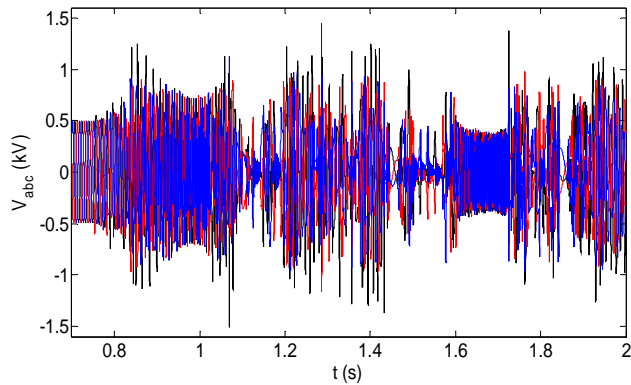


Fig. 18. Voltages at LV side of the DFIG-F104 transformer.

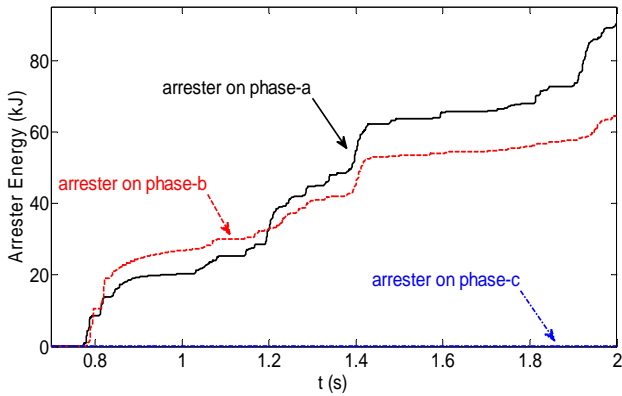


Fig. 19. DFIG- F104 transformer MV arrester energy absorption.

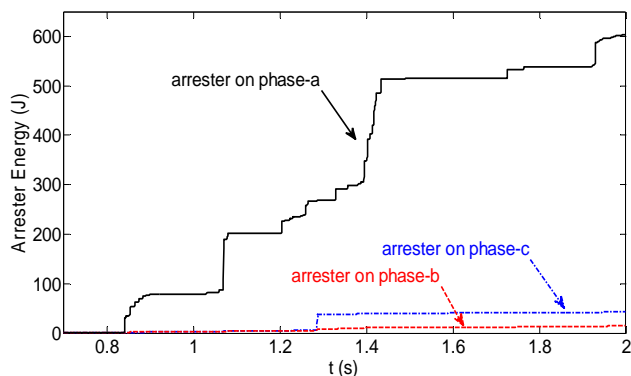


Fig. 20. DFIG- F104 transformer LV arrester energy absorption

3) Scenario S3:

In this scenario BUS2 is de-energized at 0.1 s by the operation of BUS2 CB when 34.5 kV feeders are disconnected via isolating switch. Due to unavailability of the data for the circuit breaker grading capacitances, simulations are performed for a wide range of capacitance values (50, 100, 200, 500, 1000 and 2000 pF). Ferroresonance is observed for the 2000 pF circuit breaker grading capacitance as shown in Fig. 21. It should be noted that, with 1000 pF circuit breaker grading capacitance, ferroresonance is not observed for 1.1 pu source voltage and different de-energization instants.

4) Scenario S4:

In this scenario BUS1 is de-energized at 0.1 s by the operation of wind park transformer input circuit breaker (HV CB in Fig. 8) when BUS2 is disconnected via isolating switch. The simulations are repeated for 5000, 10000, 20000, 50000 and 75000 pF circuit breaker grading capacitances. Ferroresonance is observed for the 75000 pF circuit breaker grading capacitance as shown in Fig. 22. It should be noted that, with 50000 pF circuit breaker grading capacitance, ferroresonance is not observed for 1.1 pu source voltage and different de-energization instants.

The simulations in Scenario S3 and Scenario S4 are performed to identify the critical circuit breaker grading capacitance values for the ferroresonance in the inductive voltage transformers. Therefore, the grading capacitance of HV CB is increased to very large (unrealistic) values in Scenario S4 for the ferroresonance in IVT-1.

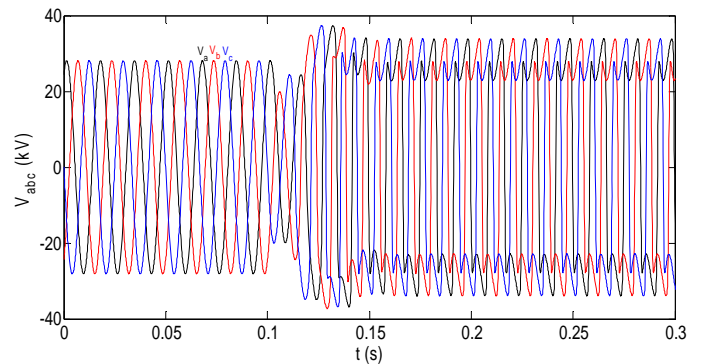


Fig. 21. Voltages at BUS2.

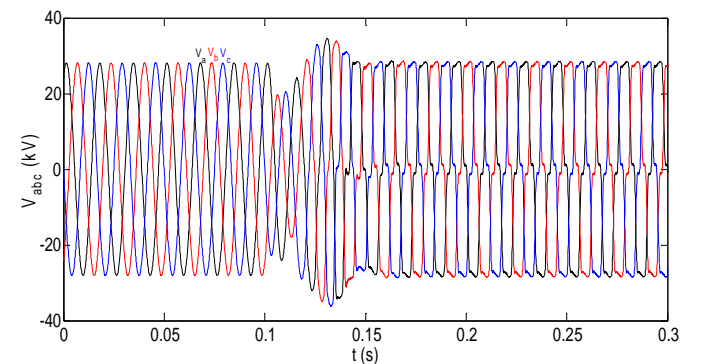


Fig. 22. Voltages at BUS1.

5) Scenario S5:

The secondary side voltages of the CVTs are shown in Fig.23, for one of the high voltage ride-through (HVRT) capability test simulations in [6]. In the presented simulation, the 120 kV bus voltage increases up to 1.4 pu for roughly 100ms following a voltage sag, and then reduces to 1 pu. As seen from Fig.23, the ferroresonant oscillations are well damped. However, when the suppression circuit of CVT is deactivated, the ferroresonant oscillations (on phase-b) remain as illustrated in Fig. 24. It should be noted that, the sampled voltage on CVT is used by the wind park controller and/or by the reactive power compensation device (if it exists). The positive sequence voltage extracted by the measuring units of these devices is shown in Fig. 25. It is obvious that, the ferroresonant oscillations without suppression circuit scenario will cause improper function of the wind park controller and/or the reactive power compensation device. However, the wind park controller can be expected to be less vulnerable to those oscillations due to its slow response.

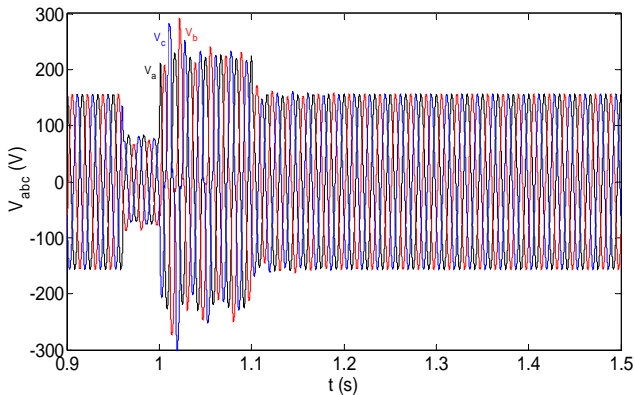


Fig. 23. Voltage at 115 kV side of the CVT (with ferroresonance suppression circuit)

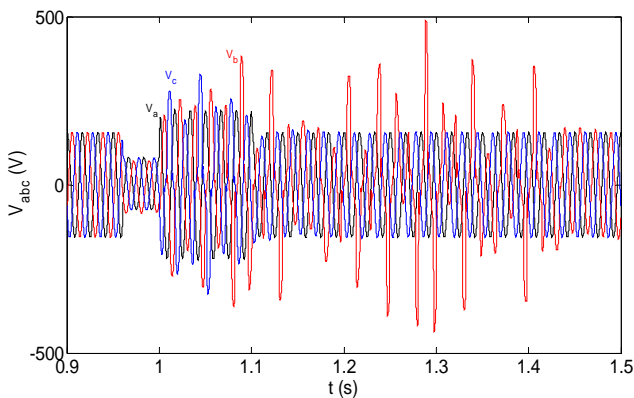


Fig. 24. Voltage at 115 kV side of the CVT (without ferroresonance suppression circuit)

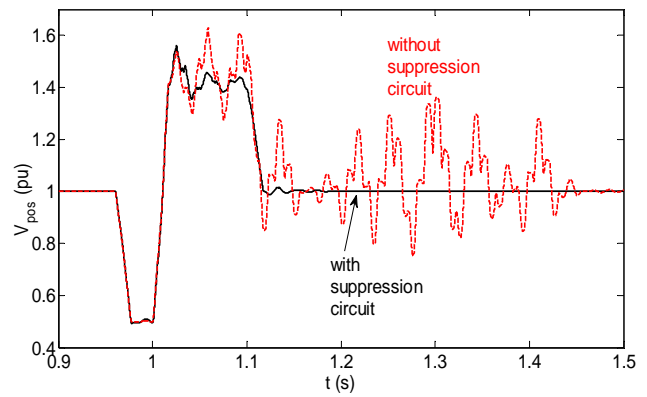


Fig. 25. Positive sequence voltage measured by the wind park controller

V. CONCLUSIONS

This paper presented the scenarios that can lead to ferroresonant circuits in an actual doubly fed induction generator (DFIG) based wind park. Ferroresonance conditions and their consequences were demonstrated by simulating the detailed model of the wind park in EMT-P-RV.

EMTP-RV simulations demonstrated that, the DFIG transformers and the collector grid may form a ferroresonant circuit when the collector grid feeder cable and large number of DFIG transformers are energized together on one or two phases (due to a stuck pole or poles in the feeder circuit breaker). However, this can be avoided with energizing the collector grid feeder cable and the DFIG transformers sequentially, i.e. following feeder energization procedure.

DFIG transformers and collector grid may also form a ferroresonant circuit with nuisance tripping of feeder overcurrent relay and a stuck pole in the feeder circuit breaker. Simulation results demonstrated that, this condition produces higher overvoltage compared to the previous one. Stuck pole in the feeder circuit breaker can be detected with “breaker pole failure relay” usage. However, the energy absorption capability of the surge arresters should be sufficient to withstand the overvoltage until the associated circuit breakers operate.

In this study the critical grading capacitance values were also identified with simulations for the ferroresonance in the inductive voltage transformers of the wind park. Depending on the manufacturer data, a ferroresonance mitigation study might be required for the inductive voltage transformers.

Simulations also demonstrated that the ferroresonance suppression circuit of CVT provides sufficient damping to ferroresonant oscillations and avoids possible improper operation of wind park and/or reactive power compensation device controller.

VI. REFERENCES

- [1] P. Ferracci, "Ferroresonance", Groupe Schneider: Cahier technique no 190, March 1998.
- [2] V. Valverde, G. Buigues, A. J. Mazón, I. Zamora, I. Albizu, "Ferroresonant Configurations in Power Systems", *International*

Conference on Renewable Energies and Power Quality (ICREPQ) Santiago de Compostela (Spain), March 2012.

- [3] M. Rioual, J. Mahseredjian, "Ferroresonance dans les réseaux – Définition, description et classification", *Les Techniques de l'Ingénieur*, May 10, 2009, Dossier D91. 9 pages.
- [4] M. Rioual, C. Kiény, J. Mahseredjian, "Ferroresonance dans les réseaux – Modélisation et applications aux typologies de circuit", *Les Techniques de l'Ingénieur*, August 10, 2009, Dossier D92, 15 pages.
- [5] E. D. Price, "Voltage Transformer Ferroresonance in Transmission Substations" proc. on *Texas A&M 30th Annual Conference for Protective Relay Engineers*, Texas A&M University, April 1997.
- [6] U. Karaagac, J. Mahseredjian, L. Cai, "High Voltage Ride-Through Capability of DFIG-based Wind Parks with FACTS" *13th International Workshop on Large-Scale Integration of Wind Power into Power Systems*, Berlin, Germany, Nov. 2014.
- [7] D. A. N. Jacobson, "Examples of ferroresonance in a high voltage power system", in *Proc. of IEEE-PES General Meeting*, 2003, pp. 1206-1212.
- [8] Hopkinson, R., "Ferroresonant overvoltage control based on TNA tests on three-phase delta-wye transformer banks", *IEEE Trans. on Power App. & Systems*, Vol. 86, No. 10, pp. 289-293, Oct. 1967.
- [9] Young, F., Schmid, R., Fergestad, P., "A laboratory investigation of ferroresonance in cable-connected transformers", *IEEE Trans. on Power App. & Systems*, Vol. 87, No. 5, pp. 1240-1249, May 1968.
- [10] Walling, R., Barker, K., Compton, T., and Zimmerman, L., "Ferroresonant overvoltages in grounded wye-wye padmount transformers with low-loss silicon steel cores", *IEEE Trans. on Power Delivery*, Vol. 8, No. 3, pp. 1647-1660, July 1993.
- [11] D. A. N. Jacobson, D. R. Swatek, and R. W. Mazur, "Mitigating potential transformer ferroresonance in a 230 kV converter station", in *Proc. of IEEE Transmission and Distribution Conference*, 1996, pp. 269-275.
- [12] D.A.N. Jacobson, and R.W. Menzies, "Investigation of Station Service Transformer Ferroresonance in Manitoba Hydro's 230-kV Dorsey Converter Station", *Proc. of 2001 Intl. Conf. on Power Systems Transients*, June 24-28, Rio de Janeiro.
- [13] L. Bolduc, B. Bouchard, and G. Beaulieu, "Capacitor divider substation", *IEEE Trans. Power Delivery*, Vol. 12, No. 3, pp. 1202-1209, July 1997.
- [14] Iravani, M.R., Wang, X., Polishcuk, I., Ribeiro, J., Sarshar, A., "Digital Time-Domain Investigation of Transient Behaviour of Coupling Capacitor Voltage Transformer", *IEEE Trans. on Power Delivery*, Vol. 13, No. 2 pp. 622-629, April 1998.
- [15] R. G. Andrei and B. R. Halley, "Voltage transformer ferroresonance from an energy transfer standpoint", *Power Delivery*, IEEE Transactions on, vol. 4, pp. 1773- 1778, 1989
- [16] S. K. Chakravarthy and C. V. Nayar, "Ferroresonant oscillations in capacitor voltage transformers", in *Proc of IEE Circuits, Devices and Systems*, vol. 142, pp. 30- 36, 1995.
- [17] M. R. Iravani, X. Wang, I. Polishchuk, J. Ribeiro, and A. Sarshar, "Digital time-domain investigation of transient behaviour of coupling capacitor voltage transformer", *Power Delivery*, IEEE Transactions on, vol. 13, pp. 622- 629, 1998.
- [18] M. Graovac, R. Iravani, W. Xiaolin, and R. D. McTaggart, "Fast ferroresonance suppression of coupling capacitor voltage transformers", *Power Delivery*, IEEE Transactions on, vol. 18, pp. 158-163, 2003.
- [19] M. Sanaye-Pasand, A. Rezaei-Zare, H. Mohseni, S. Farhangi, and R. Iravani, "Comparison of performance of various ferroresonance suppressing methods in inductive and capacitive voltage transformers", in *Proc. of IEEE Power India Conference*, 2006.
- [20] F. B. Ajaei, M. Sanaye-Pasand, A. Rezaei-Zare, and R. Iravani, "Analysis and Suppression of the Coupling Capacitor Voltage Transformer Ferroresonance Phenomenon", *Power Delivery*, IEEE Transactions on, vol. 24, pp. 1968-1977, 2009.